NUMERICAL ANALYSIS OF A HIGH SWIRL-GENERATING HELICAL INTAKE PORT FOR DIESEL ENGINES

Mirko Baratta, mirko.baratta@polito.it
Andrea E Catania, andrea.catania@polito.it
Francesco C Pesce, francesco.pesce@polito.it
Ezio Spessa, ezio.spessa@polito.it
IC Engines Advanced Laboratory, Politecnico di Torino, Italy

Horácio A Vielmo, vielmoh@mecanica.ufrgs.br
Mechanical Engineering Department, Federal University of Rio Grande do Sul, Brazil

Abstract. *This paper focuses on a steady state regime that occurs in the flow permeability and swirl generation tests of a Diesel engine intake system. The swirl generator inlet port considered is a shallow ramp helical type. The engine under consideration has a bore of 79.5 mm and a stroke of 86 mm. But in order to simulate the workbench, this last dimension was extended to 160 mm, compounding the whole calculus dominium. Numerical solutions using a commercial Finite Volumes CFD code are performed and compared with the experimental results, regarding the discharge and swirl coefficients, for diverse lifts of the intake valve. Regarding the turbulence, computations were performed with the Reynolds-Averaged Navier-Stokes, Eddy Viscosity Models k-ε cubic, in its High-Reynolds and Low-Reynolds approaches. It was also tested the RNG variant. A detailed mesh independence study was performed, arriving in submillimeter meshes, including a subsurface to assure an adequate wall treatment. For the High-Reynolds approach the subsurface has 2 layers non linearly distributed, obtaining $y^+ < 40$, and for the Low-Reynolds approach 12 layers non linearly distributed were employed, to have $y^+ < 3$. In the last case approximately a half quantity of all cells are put in the subsurface. In the same way many convergence tests were performed, and a secure criterion established. The simulations were done for diverse intake and in-cylinder pressures. The enthalpy equation is also solved, and the air compressibility is considered, being treated as a perfect gas. Thought the results it is possible to note significant divergences between the turbulence models employed, mainly in the calculated swirl coefficients. The boundary layer dynamics descriptions by the models are analyzed. The presence of recirculations in the port and in-cylinder are detected and detailed discussed.*

Keywords*: Diesel engine, high swirl-generating helical intake port, CFD, turbulence models*

1. INTRODUCTION

The detailed understanding of the flow dynamics characteristics of intake system, and mainly the in-cylinder flow, of ICE is necessary for an efficient combustion process and related emissions to the environment. Its accurate and feasible numerical simulation remains a challenge, especially in the case of swirling flows, considering the usual complexity of the geometry, the large turbulence spectra associated with the annular vortical jet after the intake valve, adding the compressible non-isothermal effects. This paper focuses on a steady state regime that occurs in the flow permeability and swirl generation tests of a Diesel engine intake system (Fiat Research Center, 1982; 1983).

During the last years more numerical simulations have been done regarding the discharge coefficient (Bianchi *et al.*, 2002; Bianchi and Fontanesi, 2003), focusing on directed intake port types, including comparisons with experimental measurements. An even more challenging situation occurs in the presence of swirl generator inlet ports of ramp helical type, including the determination of the swirl coefficient. With the growing availability of turbulence models and computational resources, many works make comparisons, regarding their capacity to reproduce experimental data and CPU time demanding.

Kaario *et al.* (2003) compared the k-ε RNG turbulence model with the one-equation subgrid scale model, incompressible and isothermal LES approach. This particularized form of the LES model used was able to capture more flow's complex structures than the k-ε RNG model, but remains the CPU large time demand problem.

Keeping the popular k-ε family, some works have analyzed the alternatives for the stress-strain relationship, considering the compressible, non-isothermal, anisotropic effects presents in the ICE three-dimensional flows.

Bianchi *at al.* (2002) compared k-ε linear and nonlinear (quadratic and cubic) eddy viscosity models, concluding that cubic stress-strain relation provided the best agreement with data, for those ICE three-dimensional flows considered. In another work Bianchi and Fontanesi (2003) investigated the High Reynolds and Low Reynolds near wall approaches, both with a cubic relationship between Reynolds stresses and strains. It was concluded that the Low Reynolds approach (boundary layer also discretized by the mesh), although increasing the computational effort, presented more ability to capture the details of the tested ICE intake flow.

An alternative is to use RNG models instead of nonlinear ones, considering its underlying concepts similar to non linear models, but with more objective simplicity. Baratta *et al.* (2003) obtained a better experimental agreement for engine flows modifying the RNG constants, presenting another valid possibility.

By these reasons the present work explores the following turbulence models: k-ε High and Low Reynolds Cubic, k-ε RNG standard and modified coefficients.

2. EXPERIMENTAL DATA

The intake system under investigation in this work is of a four-stroke compression-ignition engine, containing a swirl generator inlet port of shallow ramp helical type (Fiat Research Center, 1982; Tindal *et al.*; 1982; Favero, 2006). It is coupled with a seat valve with an inner diameter (d_V) of 31.5 mm, and outer diameter of 34.5 mm. The cylinder bore (B) is 79.5 mm, and the stroke 86 mm, although in the flow workbench, which has no piston, the cylinder dimension has been extended to 160 mm, compounding the whole calculus dominion. The compression ratio is 18:1, the maximum intake valve lift is 8.1 mm and the entire intake process occurs along a crankshaft angle interval of 240^o. The experimental measures were made according the methodology described in Fiat Research Center (1983), obtaining its discharge and swirl coefficients (Heywood, 1988). The discharge coefficient for a certain valve lift, C_{Dl} , is a relation between the real air flow rate through the intake valve ($\dot{m}_l$) and the hypothetical flow rate obtained in an isentropic expansion though the same face area ($\pi d_V^2 / 4$). For a non-choked uniform flow, caused by the expansion ratio p_{out}/p_o ,

$$C_{Dl} = \frac{\dot{m}_l}{\dfrac{\pi d_V^2}{4} \dfrac{p_o}{\left(RT_o\right)^{1/2}} \left(\dfrac{p_{out}}{p_o}\right)^{1/k} \left\{ \dfrac{2k}{k-1} \left[1 - \left(\dfrac{p_{out}}{p_o}\right)^{(k-1)/k} \right] \right\}^{1/2}} \tag{1}$$

where $\dot{m}_l$ is obtained experimentally, or from the numerical solution, in this paper.

The swirl coefficient for a certain valve lift, I_l , is a relation between the flow's angular moment with its axial moment. On the hypothesis of rigid body, for the angular velocity ω , and axial average velocity v_m ,

$$I_l = \frac{\omega \dfrac{B}{2}}{v_m} \tag{2}$$

As the real flow does not acts as a rigid body, realizing the product of the position vector and the velocity vector, and numerically calculating the axial average velocity, the Eq. (2) becomes

$$I_l = \frac{\dfrac{\int_m \left(zu - xw\right) dm}{\int_m r^2 dm} \dfrac{B}{2}}{\dfrac{\int_m v dm}{\int_m dm}} \tag{3}$$

where the integrations are made with the velocity components of the flow (*u,v,w*), for the coordinates (*x,y,z*), and corresponding radio *r*.

As the swirl movement of the air inside the cylinder varies along its axis, it is necessary to define the section where the measure is done. In this case (Fiat Research Center, 1983), the section is localized at a distance of one bore, starting from the cylinder head ($Y = 1B$). The measures were made in steady state regime, for diverse valve lifts, obtaining a pair of coefficients for each lift. Global coefficients, C_D and I_m , are obtaining by integration along the crankshaft angle θ, as follows

$$C_D = \frac{\int_{IVO}^{IVC} C_{Dl} d\theta}{IVC - IVO} \tag{4}$$

$$I_m = \frac{\int_{IVO}^{IVC} \dot{m}_l I_l d\theta}{\int_{IVO}^{IVC} \dot{m}_l d\theta} \tag{5}$$

For the present engine the experimentally obtained global coefficients are C_D = 0.372 and I_m = 2.61, with an estimated experimental error of 4%.

3. NUMERICAL METHODOLOGY

Numerical solutions using a commercial Finite Volumes CFD code (StarCD, 2006) were performed, regarding the discharge and swirl coefficients, for diverse lifts of the intake valve. User defined unstructured hexahedral-trimmed cells meshes were constructed, as showed in the Figure 1.

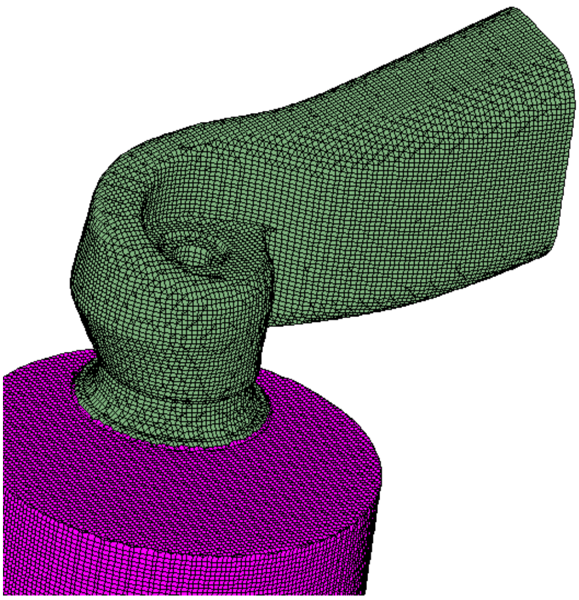

Figure 1. Unstructured hexahedral-trimmed cells mesh

In order to provide an adequate capture of the variable gradients, all the meshes were refined close to the walls, as can be seen in the Figure 2,

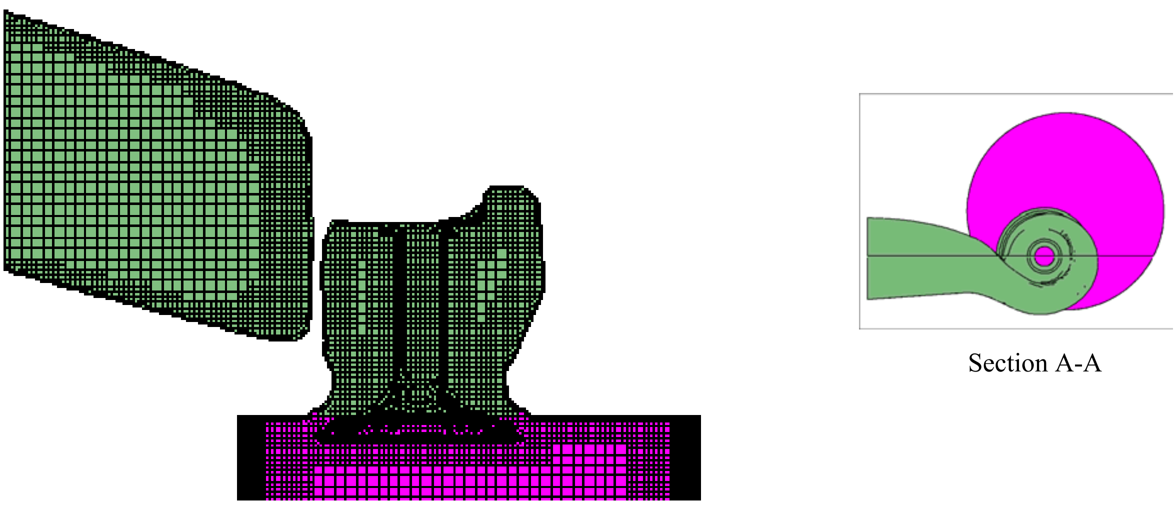

Figure 2. Section A-A mesh detail in the swirl generator intake port, valve and cylinder

A detailed mesh independence study was performed, arriving in submillimeter meshes between 485,000 and 1,064,000 cells, including a subsurface of 0.4 mm to assure an adequate wall treatment. For the High-Reynolds approach turbulence models the subsurface has 2 layers, non linearly distributed, in order to obtain $y^+ < 40$. For the Low-Reynolds approach 12 layers, non linearly distributed, were employed, to have $y^+ < 3$. In the last case approximately a half quantity of all cells are put in the subsurface. In the same way many convergence tests were performed, and a secure criterion established. All computations were performed in double precision.

To better understand the characteristics of the phenomenon, starting from the atmospheric pressure at the inlet, were simulated expansion ratios of 0.75 and 0.88. But aiming to reach an experimental validation of the results (Fiat Research Center, 1982), it was also considered a stagnation pressure of 1.1 atm at the inlet, with 293 K, discharging in an ambient pressure of 1.0 atm, and 293K. As differencing schemes were tested the Upwind Differencing (UD), the Linear Upwind Differencing (LUD) with blending factor (bf) of 0.6, and the Monotone Advection and Reconstruction Scheme (MARS) with bf = 0.5 (StarCD, 2006). For all cases the turbulence boundary conditions are turbulence intensity of 0.05 and length scale of 0.0035m, as a consequence of the flow and geometrical characteristics. The pressure-velocity coupling is solved thought the SIMPLE algorithm (StarCD, 2006). The enthalpy equation is also solved, and the air is treated as a perfect gas.

4. VALIDATION OF THE NUMERICAL SIMULATIONS

As a first step, aiming to validate the present numerical implementation, simulations were done reproducing the parameters used in the Fiat Research Center (1982; 1983) experimental apparatus: p_o = 1.1 atm, p_{out} = 1 atm, T_o = 293 K. The section for the calculus of the swirl coefficient, I_l , is localized at a distance of one bore, starting from the cylinder head ($Y = 1B$). The turbulence model used is this case is the Standard k-ε High Reynolds Cubic, Standard near wall treatment. It is applied the second order accurate Linear Upwind Difference (LUD), with a blending factor of 0.6 (StarCD, 2006). The results are described in the Tab. 1.

Table 1. Simulation's results for p_o = 1.1 atm, p_{out} = 1 atm, T_o = 293 K at $Y = 1B$
LUDbf0.6 as differencing scheme (StarCD, 2006).

Turbulence model	Intake valve lift (mm)	$\dot{m}_l$ (kg/s)	C_{Dl}	I_l
k-ε High Reynolds Cubic Std wall function	1.00 4.30 7.50	0.011719 0.043104 0.053641	0.0966 0.355 0.442	1.81 2.64 2.57

It can be seen that de C_{Dl} coefficient is more dependent of the valve lift than the I_l coefficient. This is an expected behavior, after a physical interpretation of the Eqs. (1) and (3).

The numerical integrations, defined in the Eqs. (4) and (5), are done considering a half symmetrical part (120°) of the valve lift curve of the present engine, according the Tabs.1 and 2,

Table 2. Angular interval for the numerical integrations, corresponding to each intake valve lift.

Intake valve lift (mm)	Angular interval $\Delta\theta$ (°)
1.00	18
4.30	49
7.50	53

The result of integration, and a comparison with the experimental data are shown in the Tab. 3.

Table 3. Numerical and experimental global results.

Case	C_D	I_m
Experimental (4% of accuracy)	0.372	2.61
Numerical simulation with k-ε High Reynolds Cubic Standard wall function	0.355	2.57

It is observed a good agreement with the experimental results, for both coefficients, validating the present numerical simulation. It should be considered the assumed experimental error of 4%. New explorations are made and shown in the following sections.

5. OTHER BOUNDARY CONDITION VALUES

The following investigation focus on atmospheric charged engines. By this way, differently of the situation explored in the last section, in this case p_o = 1.0 bar, and the in-cylinder suction pressure, p_{out} , is taken 0.88 and 0.75 bar. The results obtained from diverse turbulence models and differencing schemes are shown in Tab. 4. The section of the cylinder where the swirl coefficient is calculated, Y, is $0.83B$. The results of integration, according Eqs. (4) and (5), are shown in the Tab. 5.

Table 4. Simulation's results for p_o= 1.0 bar, p_{out} = 0.88 and 0.75 bar, at $Y = 0.83B$

Turbulence model	Intake valve lift (mm)	p_{out}/p_o	Diff scheme	$\dot{m}_l$ (kg/s)	C_{Dl}	I_l
k-ε High Reynolds Cubic Std wall function	1.00	0.88/1.0	UD	0.01170	0.0952	1.93
			LUDbf0.6	0.01176	0.0957	2.14
		0.75/1.0	UD	0.01493	0.0919	1.65
	4.30	0.88/1.0	UD	0.04343	0.353	2.53
			LUDbf0.6	0.04371	0.356	2.74
		0.75/1.0	UD	0.05810	0.357	2.37
	7.50	0.88/1.0	UD	0.05610	0.457	2.21
			LUDbf0.6	0.05458	0.444	2.58
		0.75/1.0	UD	0.07693	0.473	2.06
k-ε RNG Std wall function Std coefficients	1.00	0.88/1.0	LUDbf0.6	0.01260	0.1025	2.43
			MARSbf0.5	0.01262	0.1027	2.84
	4.30		UD	0.04530	0.369	2.76
			LUDbf0.6	0.04621	0.376	3.17
			MARSbf0.5	0.04705	0.383	3.49
	7.50		LUDbf0.6	0.05508	0.448	3.24
k-ε RNG Std wall funct. Modified coefficients	4.30	0.88/1.0	LUDbf0.6	0.04645	0.378	2.75
k-ε Low Rey. Cubic Std wall treatment	4.30	0.75/1.0	UD	0.05667	0.348	2.30

Table 5. Results of the integration, according Eqs. (4) and (5).

Turbulence model	p_{out}/p_o	Diff scheme	C_D	I_m
k-ε High Reynolds Cubic Std wall function	0.88/1.0	UD	0.360	2.37
		LUDbf0.6	0.356	2.63
	0.75/1.0	UD	0.369	2.18
k-ε RNG– Std wall function Std coefficients	0.88/1.0	LUDbf0.6	0.367	3.18

From the results of Tab. 4, it can be seen that the C_{Dl} coefficient is more dependent of the valve lift than the I_l coefficient. Indeed, from the Eq. (1) it is possible to see that as $\dot{m}_l$ increases with the valve lift, the C_{Dl} coefficient also increases. By the other way, the Eq. (3) does not show a clear relationship with the valve lift. The I_l coefficient presents a grater dependence of the expansion ratio and applied differencing scheme. This behavior repeats for the k-ε High Reynolds Cubic, Std wall function turbulence model, and also for the k-ε RNG, Std wall function, Std coefficients. The reason is the coupling between flow structure and the I_l coefficient.

The first order accurate differencing UD scheme is more robust than the LUD, as expected, but presents significant differences in the results, especially for the I_l coefficient.

The k-ε RNG, Std wall function, Std coefficients clearly underestimates the turbulent stresses, producing higher coefficients, especially I_l , for the second orders LUD and MARS. The k-ε RNG, Std wall function, Modified coefficients, according Baratta *et al.* (2003): $C_\mu = 0.09$; C_2=1.75; C_4=-0.373; $\sigma_k = 1$; $\sigma_\varepsilon = 1.22$, for the case tested, minimized this tendency. The MARS was the most instable scheme, especially when an increase of the blending factor is tried, arriving in situations where converge is not reached. There is a limitation also in the blending factor applied to the LUD scheme. Although it is desirable to use bf = 1, increasing the order of the differencing scheme, it was not possible to use more than 0.6, because the lack of convergence.

For the case tested, the Low Reynolds approach of the k-ε model does not produce results significantly different of that produced by the High Reynolds approach. This suggests that for the present situation the Low Reynolds approach does not justify the increase of CPU time required.

The Tab. 5 confirms the tendencies already observed in the Tab. 1: the applied turbulence models are ready to produce good results for the C_D coefficient, but the I_m coefficient presents a considerable dispersion.

The general pattern of the flow is detected by all the turbulence models tested, but the Low Reynolds approach, in addition, provides a detailed description of the boundary layer. By this reason it is selected to the following discussion, according the Figures 3, 4 and 5.

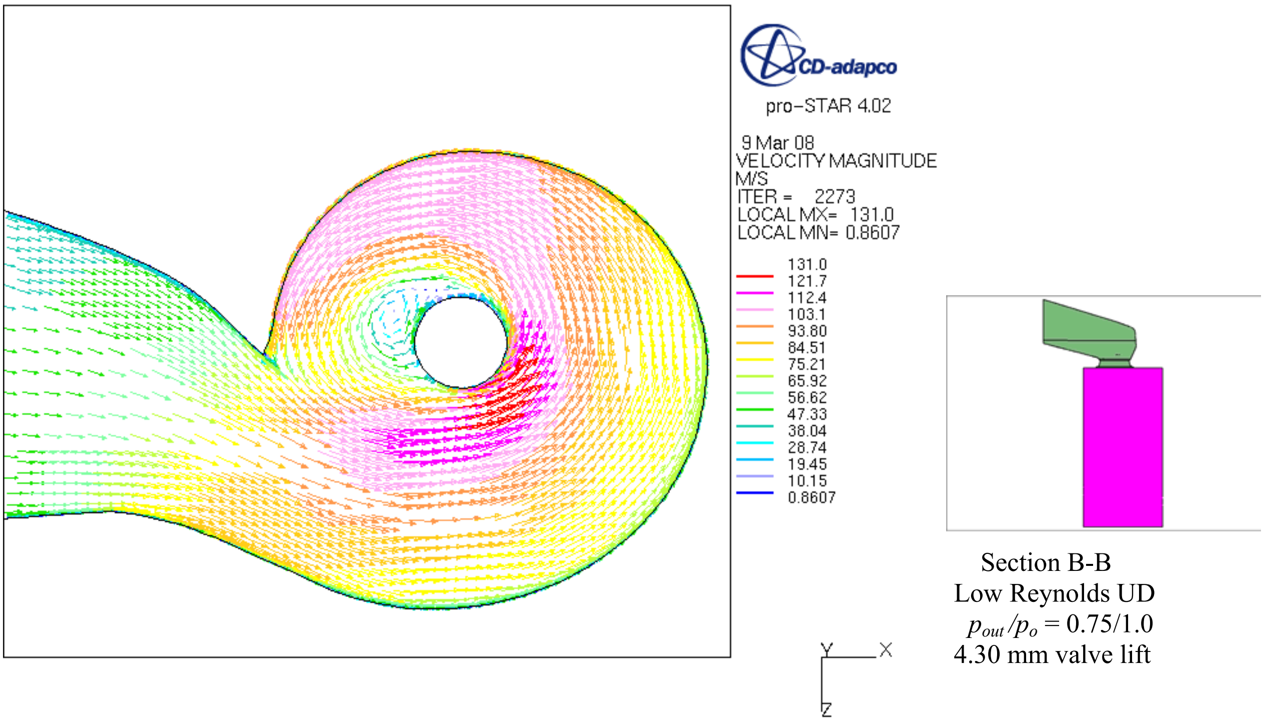

Figure 3. Velocity vectors on section B-B in the swirl generator intake port

The Figure 3 also shows the mesh concentration near the walls, arriving in the subsurface of 0.4 mm, containing 12 layers non-linearly distributed, in order to promote the Low Reynolds approach. It is detected a large recirculation flow, caused by the valve rod downstream low pressure. This high scale phenomenon is detected by all turbulence models and differencing schemes tested, for all valve lifts. It seems to be an intrinsic problem of the shallow ramp helical type swirl generator, and a potential cause for a reduction of discharge coefficient.

The Figure 4 shows velocity vectors on section A-A, in the seat valve region.

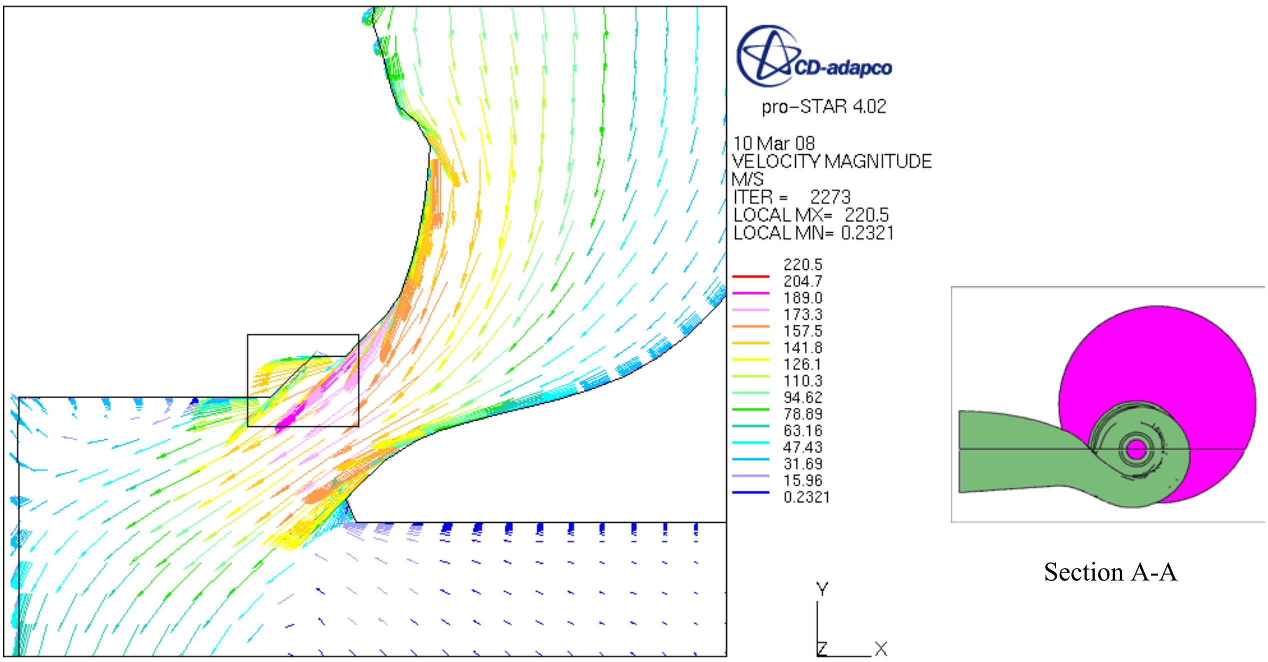

Figure 4. Velocity vectors on section A-A, in the seat valve region, for k-ε Low Re, UD, $p_{out}/p_o = 0.75/1.0$ and 4.30 mm valve lift

Because the face area restriction, this is the point of higher velocities and friction. It is possible to observe the boundary layer dynamics, including stalls caused by adverse pressure gradients. One of them is identified by the rectangle, and zoomed in the Figure 5. It is caused by the abrupt expansion immediately after the valve seat. The separation after the valve plate can also be seen, producing a complex annular helical jet, and its respective shear layer, propagating to the interior of the cylinder.

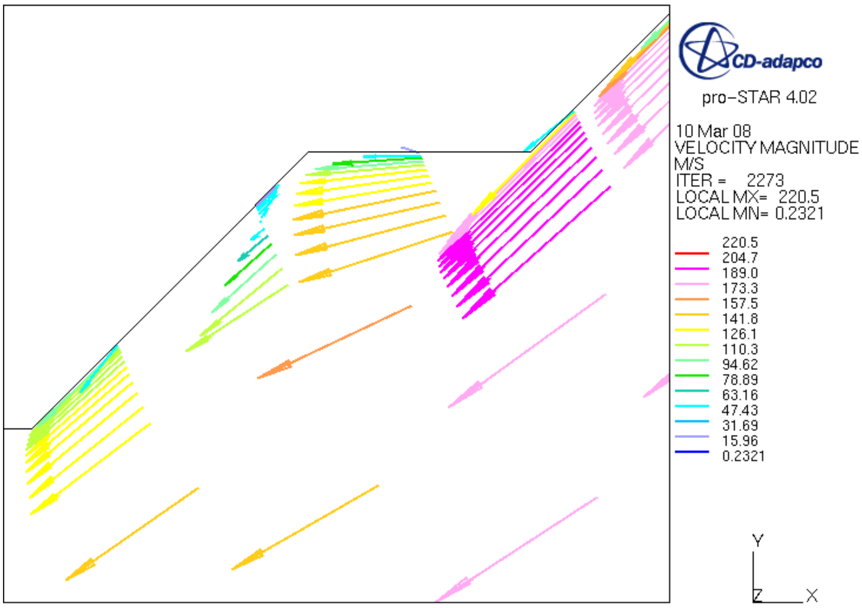

Figure 5. Detail defined in the Figure 4: a stall caused by the local expansion after the valve seat

The Figure 6 shows the velocity vectors in the section localized at $Y = 1B$, where the swirl coefficient is measured by the experimental apparatus described in Fiat Research Center (1982).

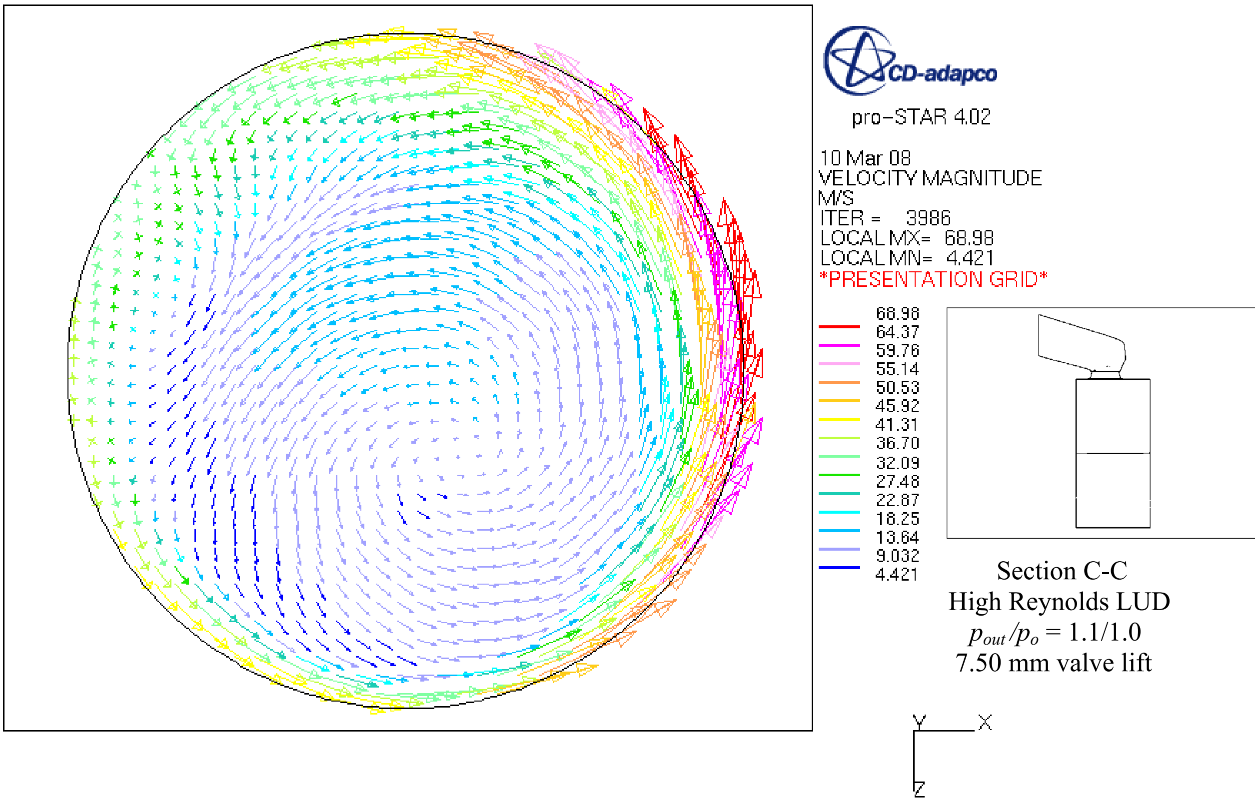

Figure 6. Velocity vectors on section C-C in the cylinder ($Y = 1B$)

As the valve is not localized at the center of the cylinder, the produced swirl is not centralized also, as can be observed. There is a lower intensity counter-vortex, causing a tangential velocity decrease in the opposite region.

6. CONCLUSIONS

For the pressure relation p_{out}/p_o of 1.0/1.1, considering both the coefficients, the k-ε High Reynolds Cubic presents a major agreement with the experimental results, validating the present numerical simulation. The k-ε RNG Std wall function, modified coefficients performs even better for the C_D coefficient, but the I_m presented an excessive growing.

For the pressure relation p_{out}/p_o of 0.88/1.0 and 0.75/1.0, the I_m coefficient results present significantly divergences among the turbulence models and differencing schemes employed. By the other way, acceptable results were obtained for C_D coefficient.

The presence of recirculations in the port and in-cylinder are detected and discussed. The boundary layer dynamics is well detected by the Low Reynolds approach.

7. ACKNOWLEDGMENTS

The authors thank the financial support from CAPES-Brazil through a post-doctorate scholarship grant to Vielmo, H.A.

8. REFERENCES

Baratta, M., Catania, A.E., Spessa, E., and Liu, R.L., 2003. "Multidimensional Predictions of In-Cylinder Turbulent Flows: Contribution to the Assessment of k-ε Turbulence Model Variants for Bowl-In-Piston Engines". ASME J. of Eng. Gas Turbines Power, 127, pp. 883-896.

Bianchi, G.M., Cantore, G. and Fontanesi, S., 2002. "Turbulence Modeling in CFD Simulation of ICE Intake Flows: The Discharge Coefficient Prediction". SAE Paper N^o 2002-01-1118.

Bianchi, G.M., Cantore, G., Parmeggiani, P. and Michelassi, V, 2002. "On Application of Nonlinear k-ε Models for Internal Combustion Engine Flows". Transactions of the ASME vol. 124, pp. 668-677.

Bianchi, G.M., Fontanesi, S., 2003. "On the Applications of Low-Reynolds Cubic k-ε Turbulence Models in 3D Simulations of ICE Intake Flows". SAE Paper N^o 2003-01-0003.

Favero, F., 2006. "Tecniche di Modellazione e di Analisi Numerica per lo Studio del Moto della Carica in Camera di Combustione e loro Applicazione ad un Motore Diesel ad Elevato Swirl". Thesis, IC Engines Advanced Lab, Politecnico di Torino, Italy, (in italian).

Fiat Research Center; Consiglio Nazionale delle Ricerche, 1982. " Motore Monocilindro Diesel con Distribuzione a 2 Valvole e Protezioni Termiche Camera di Combustione". Contract N^o 82.00047.93 (in italian).

Fiat Research Center; Consiglio Nazionale delle Ricerche, 1983. "Metodologia per la Caratterizzazione dei Condotti di Aspirazione Motori in Flusso Stazionario". Contract N^o 82.00047.93 (in italian).

Heywood, J.B., 1988. "Internal Combustion Engines". McGraw-Hill Inc.

Kaario, O., Pokela, H., Kjaldman, L., Tiainen, J. and Larmi, M., 2003. "LES and RNG Turbulence Modeling in DI Diesel Engines". SAE Paper N^o 2003-01-1069.

StarCD User Guides, 2006. CD-adapco.

Tindal, M.J., Williams, T.J., Aldoory, M., 1982. "The Effect of Inlet Port Design on Cylinder Gas motion in Direct Injection Diesel Engines". ASME, Flows in Internal Combustion Engines, pp. 101-111.

9. RESPONSIBILITY NOTICE